Early functional and cognitive declines measured by auditory evoked cortical potentials in Alzheimer's disease mice

Ling Mei*, Li-Man Liu*, Kaitian Chen, Hong-Bo Zhao

Department of Otolaryngology, University of Kentucky Medical Center, 800 Rose Street, Lexington, Kentucky, USA, 40536

* Equal contributors

Running title: Declining of AECP in AD mice

Corresponding Author:

Hong-Bo Zhao, Ph.D./M.D.
Professor
Dept. of Otolaryngology
University of Kentucky Medical Center
800 Rose Street
Lexington, KY 40536 – 0293
USA
Tel: 859-257-5097 x 82138
Fax: 859-257-5096
E-mail: hzhao2@uky.edu

Abstract

Alzheimer's disease (AD) is characterized with a progressive loss of memory and cognitive decline. Early detection of AD is critical for prevention and intervention of this common neurodegenerative disease. Previous studies demonstrated that auditory dysfunction could occur at the early stage of AD. Auditory evoked cortical potential (AECP) is an event-related potential reflecting not only neural activation in the auditory cortex but also cognitive activity in the brain. In this study, we recorded AECP in AD mice. AECP in mice usually possessed 3 waveforms. The early sensory P1 and P2 peaks were clearly visible in 1 month old mice. However, the later cognitive P3 peak was not well-developed until the age of 3 months old. In APP/PS1 AD mice, P1 and P2 were reduced at young ages (<6 months old), prior to occurrence of AD phenotypes. Different from normal aging, the cognitive peak of P3 in AD mice was diminished invisible after 4 months old. The latencies of peak N1, P2, and N2 in AD mice before 3 months were shorter than those in WT mice. Consistent with AECP changes, expression of amyloid precursor protein (APP) was visible in the AD mouse auditory cortex at 2 months old. These data indicate that AECP has significant changes in young AD mice and can serve as an early, non-invasive, objective biomarker in AD and AD-related dementia detection and diagnosis.

Keywords: hearing; AECP; SCR; Alzheimer's disease; dementia; auditory cortex; early AD biomarker; preclinical AD; age-related hearing loss; mouse

Introduction:

Alzheimer's disease (AD) is a progressive neurodegenerative disease, characterized by a progressive loss of memory and dementia. Currently, the prevalence of AD is increasing rapidly in the United States and world. It is estimated that there will be 13.8 million AD patients in the United States by the year 2050, almost triple the 4.7 million patients in 2010 (Hebert et al., 2013). This will produce a big, heavy economic and social burden. Early detection is critical for prevention and interventions of this common neurodegenerative disease. For example, early diagnosis and interventions delaying the onset of dementia by even one year could decrease the worldwide prevalence of dementia by 10%. However, so far, the early detection of AD is still a big challenge, since lack of the early, reliable, and easily recordable AD biomarkers. In particular, cognitive decline is most common and predominant symptom at the early AD stage. Currently, it lacks objective, reliable, and measurable biomarkers to assess cognitive decline or AD-related dementia (ADRD) progressing at the early stage.

Recently, increasing evidence suggests that defects in sensory systems, including the olfactory, visual, or auditory systems, are highly associated with AD progressing (Murphy, 2019; Rochoy et al., 2019). AD pathology could appear in sensory associated areas before appearing in regions involving memory, such as the entorhinal and hippocampal areas. These neuropathological changes in the sensory associated areas can occur before cognitive symptoms become apparent. Hearing is an important neural sense. AD can cause hearing loss; hearing loss also can in turn accelerate and exacerbate AD and dementia generation (Morrison et al., 2018; Griffiths et al., 2020). Our previous study

demonstrated that auditory brainstem response (ABR), which reflects the function and integrity of the auditory pathway in the brainstem, appeared apparent reduction in APP/PS1 AD mice at 3 months old (Liu et al., 2020), prior to the occurrence of spatial learning deficit in this AD mouse model by age of 6-7 months old (Reiserer et al., 2007; Ordonez-Gutierrez et al., 2015, 2016). Recent studies also demonstrated that AD could cause auditory functional changes. It has been reported that the 5xFAD mice have early onset of deficits in auditory gap detection (Kaylegian et al., 2019; Weible et al., 2020). These studies suggest that AD could cause hearing function decline at the early stage.

In comparison with other sensory systems, the auditory system has the advantage that decline in function over time in different nuclei (centers) can easily be repeatedly, quantitatively measured and located by recordings of auditory evoked potentials. Auditory evoked cortex potential (AECP) is an auditory evoked potential recorded on the scalp surface, reflecting the neural activity of auditory cortex and related brain areas. In particular, its later waveforms reflect cognitive processing (Sur and Sinha, 2009). In this study, we recorded AECP in APP/PS1 AD mice to assess AD-induced functional changes in the auditory cortex and brain. We found that AECP in AD mice could have significant reduction at young ages. In particular, later cognitive peak P3 was diminished invisible in AD mice. Our study suggests that AECP recording could serve as a non-invasive, easily recordable, and repeatable method to assess AD and ADRD development and progression at the early stage.

Materials and Methods:

APP/PS1 AD mice and CBA/CaJ normal aging mice

APP/PS1 transgenic mice are a common, widely used AD mouse model and were used in this study. APP/PS1 AD mice were purchased from Jackson Laboratory, USA (Stock No: 004462, mixed C57BL/6;C3H genetic background). After received, we crossed them with CBA/CaJ mice (Stock No: 00654, Jackson Laboratory, USA). APP/PS1 transgenic mice possess both chimeric mouse/human amyloid precursor protein (Mo/HuAPP695swe) and mutant human presenilin 1 (PS1-dE9) (Reiserer et al., 2007). Based on Jackson Laboratory's technical notice, APP/PS1 transgenes were detected by PCR amplification of tail genomic DNA using the following primers: wild-type (WT) forward: 5'-GTG TGA TCC ATT CCA TCA GC- 3'; Common: 5'-GGA TCT CTG AGG GGT CCA GT- 3'; Mutant forward: 5'-ATG GTA GAG TAA GCG AGA ACA CG- 3'. Mutant and WT mice generated 142 and 265 bps bands, respectively. WT littermates served as controls. CBA/CAJ mice were also used for normal aging study. All experiments and procedures were approved and conducted in accordance with the policies of the University of Kentucky Animal Care & Use Committee (approved protocol #: UK00902M2005).

Auditory evoked cortical potential recording

Auditory evoked cortical potential (AECP) was recorded in a double-wall sound isolated chamber by use of a Tucker-Davis R3 system with an ES-1 high-frequency speaker (Tucker-Davis Tech. Alachua, FL). Mice were anesthetized by intraperitoneal injection with a mixture of ketamine and xylazine (8.5 ml saline+1 ml Ketamine+0.55 ml

Xylazine, 0.1 ml/10 g). Body temperature was maintained at 37–38°C by placing anesthetized mice on an isothermal pad. Two subdermal needle electrodes were punched into the head skin at the vertex and ventrolaterally to the right or left ear. The ground needle electrode was inserted to the right leg. Cortical potentials were evoked by clicks (85 dB SPL) in alternative polarity with stimulating rate of 1/s. The recording time window was 800 ms. The signal was amplified by 50,000 and averaged by 200 time. The recording filter was set at 0 to 3 kHz. The signals were further post-filtered with a 10-order digital Gaussian filter with 12.5 Hz of central frequency and 2 Oct bandwidth for analysis.

Brain preparation and slicing

Mice were anesthetized by intraperitoneal injection with a mixture of Ketamine and Xylazine (a stock solution: 8.5 ml saline + 1 ml Ketamine + 0.55 ml Xylazine) given at a dose of 0.1 ml/10 g body weight. The anesthetized mouse was intracardially perfused with 4% paraformaldehyde for 15-20 min. Then, the mouse skull was opened. The brain was carefully removed and incubated in 4% paraformaldehyde overnight for post-fixation. Following infiltration with 30% glucose for three day with changing solution at each day, the brain was embedded in OCT (Cat # 4583, Sakura Finetek USA Inc. CA) at room temperature for one day. The embedded brain was frozen at -80ºC overnight and cut 20 µm thick at -22~24 ºC by a cryostat (Thermo Electron Corp. Waltham, MA). The tissue sections were directly mounted onto glass slides for staining and storage.

Immunofluorescent staining

Immunofluorescent staining was performed as described in our previous reports (Zhao and Yu, 2006; Wang et al., 2009). After 1 hr of incubation with the blocking solution (10% goat serum and 1% BSA in PBS) with 0.5% Triton X-100 at room temperature, the brain slides were incubated with primary antibody rabbit monoclonal anti-amyloid precursor protein (APP) [clone Y188] (#AB32136, Abcam, USA; 1:500) in blocking solution overnight. After washout with PBS three times, the brain slides were incubated with corresponding secondary antibody conjugated with Alexa Fluor-568 (Thermo Fisher Sci, USA) for 2 hr at room temperature. At the last 15 min, 4', 6-diamidino-2-phenylindole (DAPI, 0.1 mg/ml, D1306; Molecular Probes) was added into the incubation solution to visualize cell nuclei. After completely washing out the second antibodies with PBS, the sections were mounted with a fluorescence mounting medium (H-1000, Vector Lab, CA) and observed under a Nikon A1R confocal microscope system. The AD and WT mouse sections were simultaneously stained to avoid variable staining intensities and observed with the same parameters.

Data processing, statistical analysis, and reproducibility:

The amplitude and latency of peaks in AECP were measured by a house-made program with MATLAB (Mathworks Inc. USA). Data were plotted by SigmaPlot and statistically analyzed by SPSS v25.0 (SPSS Inc. Chicago, IL). Data were expressed as mean ± s.e.m. Student t tests or one-way ANOVA were performed. The threshold for significance was $\alpha = 0.05$. Bonferroni post hoc test was used in ANOVA. The recordings were at least repeated three times with different mouse groups and averaged.

Results:

Auditory evoked cortex potential (AECP) in mice

While recording of AECP is common in humans, little is recorded in mice. We first characterized AECP in mice. In mice, AECP usually appears 3 positive peaks, i.e., P1, P2, and P3, with corresponded three N1, N2, and N3 negative peaks (Fig. 1). Peak P1 and P2 could be clearly visible in recordings. However, P3 in mice was not visible until 3 months old (Fig. 1A&B). At 6 months old, AECP was well-developed and P1, P2, and P3 peaks were clearly visible (Fig. 1C). The latencies of peaks P1, P2, and P3 were 12.5±2.08, 67.5±2.74, and 128.1±6.76 ms, respectively (Fig. 2A).

Fig. 1

The effect of normal aging on AECP in mice

We further investigated the effect of normal aging on AECP in CBA/CAJ mice, which have no apparent age-related hearing loss (Zheng et al., 1999). Fig. 1 shows that AECPs were reduced with age increased. Quantitative measure shows that the amplitudes of early waveforms (i.e., P1, N1, and P2) were 4.66±0.70, -4.73±0.71, and 3.15±0.75 μV, respectively, at 1 year (12 months) old and 3.39±0.77, -3.98±0.78, and 3.41±0.86 μV, respectively, at 1.5 year (18 months) old. They had significant reduction in comparison with those at 6 month old (Fig. 2C&D). However, the amplitudes of peaks N2, P3, and N3 in later waveforms had no significant reduction with aging (Fig. 2C&D). There were no significant changes in P1 and N1 latencies. However, the latencies of P2, N2, and P3 peaks in later waveforms were significantly reduced at 12 months old (Fig. 2B).

Fig. 2

AECP in APP/PS1 AD mice

In order to assess AD-induced functional changes in the auditory cortex, we recorded AECP in AD mice. Fig. 3 shows AECP in APP/PS1 AD mice. In general, P1 and P2 in AD mice appeared smaller than those in WT littermate mice at young ages (<7 months old). At 1-3 months old, peak P2 in APP/PS1 AD mice was split (indicated by blue arrows in Fig. 3A&B). P3 is clearly visible in WT mice after 4 month old, but not visible in AD mice (Fig. 3D-I). Later negative peaks N2 and N3 in APP/PS1 AD mice were also not clearly visible in AECP recordings (Fig. 3D-I).

Fig. 3

Changes of AECP in APP/PS1 mice with aging

To assess dynamic changes with aging, we quantitatively analyzed AECP recordings. Quantitative measure shows that of AECP waveforms in APP/PS1 mice had significant changes with aging (Fig. 4). Peaks in AD mice generally appeared smaller than those in WT mice at the same age. The reduction of early peaks P1 and P2 in AD mice was significant at 4-7 months old (Fig. 4A&C). Later cognitive peak P3 in AD mice was significantly smaller than that in WT mice after 4 month old (Fig. 4E). In comparison with apparent changes in positive peaks in AD mice, the reduction in negative peaks in

AD mice was not significant, except at 10-12 months old, at which N2 and N3 peaks in AD mice had significant reduction in comparison with those in WT mice (Fig. 4D&F).

Fig. 4

The latencies of AECP peaks in AD mice usually appeared reduced or no changes except peak N2 at 12 months old (Fig. 5). The latencies of N1, P2, and N2 peaks in AD mice at 1-2 months old were significantly shorter than those in WT mice (Fig. 5B-D). Also, the latencies of P1 and N3 in AD mice at 10-12 months old appeared shorter than those in WT mice (Fig. 5A&F). However, the latency of N2 in AD mice at 12 months old was longer than that in WT mice (Fig. 5D). There were no significant changes in P3 latency between AD and WT mice in any tested ages (Fig. 5E).

Fig. 5

We further compared the AECP changes in AD mice, WT littermate mice, and CBA/CaJ mice with aging (Fig. 6). AECP changes in WT littermates with aging resembled those in CBA/CaJ mice. However, early waveforms P1, N1, and P2 in AD mice had significant reduction at young ages (3 and 6 months old in Fig. 6A-C). Also, the later waveforms of N2, P3, and N3 in AD mice were significantly reduced at 6-12 months old (Fig. 6D-F).

Fig. 6

Expression of amyloid precursor protein in the auditory cortex of APP/PS1 AD mice

Amyloid precursor protein (APP) is an AD protein. Finely, we examined APP expression in the auditory cortex and other brain areas in APP/PS1 AD mice with different ages (Fig. 7). Immunofluorescent staining shows the positive labeling of APP visible in the auditory cortex in APP/PS1 mice as early as 2 months old (Fig. 7B&E). As age increased, the deposition of APP in the auditory cortex was increased. At 12 months old, the typical APP plaque deposition pattern was visible in the auditory cortex (Fig. 7A&D). The early expression of APP in the auditory cortex is consistent with early appearance of changes in AECP recording in APP/PS1 AD mice at young ages (Figs. 4-6).

Fig. 7

Discussion:

In this study, we recorded AECP in mice and characterized changes of AECP in APP/PS1 AD mice with aging. We found that different from humans, AECP in mice usually only had three waveforms (Fig. 1). Also, P3 peak in mice was not visible until 3 months old (Fig. 1B). As age increased, the early peaks (P1, N1, and P2) in AECP were reduced, while later peaks (i.e. N2, P3 and N3) had no significant changes (Figs. 1-2). In APP/PS1 AD mice, P1 and P2 at young ages (<8 months old) appeared small in comparison with WT mice (Figs. 3-4, and 6). Peak P2 in AD mice at 1-2 months old also appeared split (Fig. 3A&B). In particular, the later 'cognitive' peak P3 in AD mice was diminished (Fig. 3) and significantly reduced with aging in comparison with that in WT littermate mice and CBA/CaJ mice (Figs. 4 and 6). However, there was no significant delay of peak latencies in AD mice, except N2 at 12 months old (Fig. 5). Actually, the latency of N1, P2, and N2 peaks at 1-2 months old and the latencies of P1 and N3 at 10-12 months old in AD mice were significantly reduced in comparison with those in WT mice (Fig. 5). Consistent with early changes in the AECP, the expression of APP AD proteins could be found in the auditory cortex in the AD mice as early as 2 months old (Fig. 7). These data suggest that AECP recording could serve as an early biomarker to detect and assess the AD generation and development.

AECP is an event-related potential reflecting the summation of post-synaptic potentials that are time-locked to certain events of interest. In humans, AECP consists of several waveforms and are named as P1 (P50), N1 (N100), P2 (P200), N2 (N250), P3 (P300), and P4 (P600) based on their latencies (Swords et al., 2018). Early waveforms

(i.e., P1 & P2) are "sensory", largely depending on the stimulus and activities in the auditory cortex; later waveforms (i.e., P3 & P4) are "cognitive" reflecting cognitive processing (Sur and Sinha, 2009). Thus, unlike other stimulus-evoked responses, the AECP recording can reflect not only the neural activities in the auditory cortex but also cognitive activities in the brain.

Although AECP is a common and traditional recording in humans, little is recorded in mice. In this study, we found that AECP could be clearly evoked in mice by click stimulation. However, in comparison with the AECP recorded from humans, AECP in mice usually only has 3 waveforms (Fig. 1). Also, in comparison with the latencies of P1, P2, and P3 in humans at ~50, 200, and 300 ms, respectively (Swords et al., 2018), the latencies of P1, P2, and P3 in mice were much shorter and 10-15, 65-70, and 110-150 ms, respectively (Fig. 2A&B). This is because mouse brain size is small and the neural interactions are less than humans. In addition, P3 in mice was not well-developed until 3 months old (Fig. 1). As mentioned above, later responses of AECP reflect cognitive processing (Sur and Sinha, 2009). Specifically, P3 is dependent on internal thought process and is considered to be mainly generated by the hippocampus where short-term memory functions are stored. These data suggest that cognitive activity in mice may need longer time to be matured during mouse postnatal development.

In APP/PS1 AD mice, early sensory P1 and P2 peaks in AECP at young ages (<8 months old) appeared small in comparison with those in WT mice (Figs. 3-4, and 6). Peak P2 in AD mice at 1-2 months old was also split (Fig. 3A-B). These data

demonstrated that AD could cause functional changes in the auditory cortex at the early stage. In previous study, we reported that hearing loss measured as ABR threshold in APP/PS1 AD mice could occur as early as 2-3 months old (Liu et al., 2020). The significant reduction of ABR peaks IV and V (which are generated by neural activities of inferior colliculus, nuclei of lateral lemniscus, and medial geniculate body in the upper brainstem) in the APP/PS1 AD mice could be found at 3 months old (Liu et al., 2020). It was also reported that the 5xFAD mice have early onset of deficits in auditory gap detection, which could be detectable at about 2 months old and became progressive worse afterwards (Kaylegian et al., 2019; Weible et al., 2020). These data demonstrated that dysfunctions of hearing occurred much earlier than the appearance of typical AD phenotypes, such as spatial learning deficit, in APP/PS1 AD mice by 6-7 months of age (Reiserer et al., 2007; Ordonez-Gutierrez et al., 2015, 2016). It has been reported that auditory sensory and cognitive cortical potentials in AD persons could be abnormal approximately 10 years before AD becomes apparent (Golob et al., 2009). Thus, AECP recording as ABR recording (Liu et al., 2020) and other hearing function tests could provide important information about AD development and progressing in the early stage, and can provide a simple, sensitive, non-invasive, and repeatable assessment for early AD detection.

We found that expression of APP in the auditory cortex could be visible as early as 2 months old (Fig. 7B&E). Based on our knowledge, there is no report yet about AD protein expression in the auditory cortex in AD transgenic mice. Previous studies in AD patients demonstrated that characterized AD pathological changes (Aβ plaques, tau

protein aggregation, and neural degeneration) in the human auditory system (Sinha et al., 1993). It was reported that positive Aβ plaques and tau proteins were identified in the auditory centers (nuclei) in the human brainstem and auditory cortex in the old AD patients (Ohm and Braak, 1989; Sinha et al., 1993; Baloyannis et al., 2007, 2009). Our result is consistent with these previous reports. A typical APP plaque deposition could be visible in the auditory cortex (Fig. 7A&D). Moreover, we further found that AD proteins could occur in the auditory cortex in AD mice at the 2 months old (Fig. 7B&E), consistent with early changes in AECP in APP/PS1 AD mice (Figs. 3-6). These findings provide further morphological evidence that AD could occur in the auditory system at the early stage.

The previous studies found that AD patients could have difficulty with dichotic listening (Grimes et al., 1985; Mohr et al., 1990; Strouse et al., 1995), understanding speech in the presence of background noise (Kurylo et al., 1993; Gates et al., 1995), impairment in hearing sensitivity (Strouse et al., 1995; Iliadou and Kaprinis, 2003), and impaired sound location (Strouse et al., 1995; Gates et al., 2002, 2011). However, there were conflicted results in previous studies, since most of those tests are based on subjective selections, which largely depends on personal cognitive conditions. Moreover, AD or aged persons have cognitive decline or dementia (Gate et al., 1995). This also makes that those subjective-dependent functional tests are hard to be performed in AD or old persons and the obtained results are hard to be interpreted. In this study, we found that P3 in AECP was significantly reduced in AD mice (Figs. 3, 4 and 6). As mentioned above, the peak P3 in AECP reflects cognitive neural processing. Thus, AECP recording

can provide an easily, non-invasive, objective test to detect and assess development and progression of AD, particularly AD-related dementia.

In this study, we also investigated normal aging effect. In normal aging CBA/CaJ mice, early waveforms (P1, N1, and P2) in AECP had significant reduction as age increased, whereas later waveform peaks N2, P3, and N3 had no significant reduction with aging (Figs. 1 and 2C&D). In AD mice, P1 and P2 were also reduced with aging (Figs. 3-4). However, in comparison with the reduction by normal aging in CBA/CaJ mice, the reduction of early peaks (P1, N1, and P2) in AD mice were more significant (Fig. 6). Also, P3 in APP/PS1 AD mice was diminished (Figs. 3, 4, and 6), while P3 in normal aging mice had no significant changes (Figs. 1 and 2). This is consistent with previous reports that AD patients had changes in amplitude of auditory evoked potentials in humans (Buchwald et al., 1989; Irimajiri et al., 2005; Swords et al., 2018); changes of cognitive N200 and P300 waves in AECP in AD patients (i.e., N2 and P3 peaks in mice) were reduced, distinguished from the effect of normal aging (Morrison et al., 2018). Thus, AECP recording could serve as a valuable clinical tool for AD diagnosis.

In mice, the latencies of peaks in AECP appeared reduced with normal aging (Fig. 2B). Moreover, there were no significant delay in peak latencies of AECP in AD mice, except peak N2 at 1 year old (Fig. 5). Actually, the latencies of peak N1, P2, and N2 at 1-2 months old (Fig. 5B-D) and the latencies of P1 and N3 at 10-12 months old in AD mice (Fig. 5A&F) were shorter than those in WT mice. This may arise from the fact that the neural interactions in AD mice are less than those in WT mice due to degeneration.

Currently, more and more AD mouse models are available. They provide useful animal models to study AD pathological mechanisms, develop therapeutic interventions, and assess the treatment efficiency. However, as mentioned above, it currently lacks objective, reliable, easily recordable biomarkers to assess AD phenotypes, particularly cognitive decline in animals. In this study, we found that AECP in AD mice was reduced (Figs. 3, 4 and 6), consistent with AECP recording in humans (Swords et al., 2018). In particular, cognitive peak P3 of AECP in AD mice was diminished, different from normal aging effect (Figs. 3, 4, and 6). These findings indicate that AECP recording could provide an easily recordable and repeatable objective method to assess AD-induced pathological changes and cognitive decline in mice. This will greatly facilitate AD studies by use of AD animal models.

Acknowledgement: This work was supported by NIH R01 DC 017025 and DC 017025-01S1 to HBZ.

Author Contributions:

HBZ conceived the general framework of this study. ML, LML, KC and HBZ performed the experiments. ML, LML, and HBZ analyzed data. HBZ wrote the paper. All authors reviewed the manuscript and provided the input.

Conflict of Interest:

The authors declare no competing interests.

References:

Baloyannis SJ, Costa V, Mauroudis I, Psaroulis D, Manolides SL, Manolides LS. (2007) Dendritic and spinal pathology in the acoustic cortex in Alzheimer's disease: morphological and morphometric estimation by Golgi technique and electron microscopy. Acta Otolaryngol. 127: 351-4. doi: 10.1080/00016480601126986.

Baloyannis SJ, Mauroudis I, Manolides SL, Manolides LS (2009) Synaptic alterations in the medial geniculate bodies and the inferior colliculi in Alzheimer's disease: A Golgi and electron microscope study. Acta Otolaryngol 129, 416–418.

Buchwald JS, Erwin RJ, Read S, Van Lancker D, Cummings JL (1989) Midlatency auditory evoked responses: Differential abnormality of P1 in Alzheimer's disease. Electroencephalogr Clin Neurophysiol 74, 378–384.

Gates GA, Anderson ML, McCurry SM, Feeney MP, Larson EB (2011) Central auditory dysfunction as a harbinger of Alzheimer dementia. Arch Otolaryngol Head Neck Surg 137, 390–395.

Gates GA, Beiser A, Rees TS, D'Agostino RB, Wolf PA (2002) Central auditory dysfunction may precede the onset of clinical dementia in people with probable Alzheimer's disease. J Am Geriatr Soc 50, 482–488.

Gates GA, Karzon RK, Garcia P, Peterein J, Storandt M, Morris JC, Miller JP (1995). Auditory dysfunction in aging and senile dementia of the Alzheimer's type. Arch Neurol 52, 626–634.

Golob EJ, Ringman JM, Irimajiri R, Bright S, Schaffer B, Medina LD, Starr A. (2009) Cortical event-related potentials in preclinical familial Alzheimer disease. Neurology. 73(20):1649-55.

Golub JS, Luchsinger JA, Manly JJ, Stern Y, Mayeux R, Schupf N. (2017) Observed Hearing Loss and Incident Dementia in a Multiethnic Cohort. J Am Geriatr Soc. 65(8):1691-1697. doi: 10.1111/jgs.14848.

Griffiths TD, Lad M, Kumar S, Holmes E, McMurray B, Maguire EA, Billig AJ, Sedley W. (2020) How can hearing loss cause dementia? Neuron. 108(3):401-412. doi: 10.1016/j.neuron.2020.08.003.

Grimes AM, Grady CL, Foster NL, Sunderland T, Patronas NJ (1985) Central auditory function in Alzheimer's disease. Neurology 35, 352–358.

Hebert LE, Weuve J, Scherr PA, Evans DA. (2013) Alzheimer disease in the United States (2010-2050) estimated using the 2010 census. Neurology. 80(19):1778-83.

Iliadou V, Kaprinis S. (2003). Clinical psychoacoustics in Alzheimer's disease central auditory processing disorders and speech deterioration. Ann. Gen. Hosp. Psychiatry 2:12. doi: 10.1186/1475-2832-2-12.

Irimajiri R, Golob EJ, Starr A (2005) Auditory brain-stem, middle-and long-latency evoked potentials in mild cognitive impairment. Clin Neurophysiol 116, 1918–1929.

Kaylegian K, Stebritz AJ, Weible AP, Wehr M. (2019) 5XFAD Mice Show Early Onset Gap Detection Deficits. Front Aging Neurosci. 11:66. doi: 10.3389/fnagi.2019.00066.

Kurylo DD, Corkin S, Allard T, Zatorre RJ, Growdon JH (1993) Auditory function in Alzheimer's disease. Neurology 43, 1893–1899.

Liu Y, Fang S, Liu LM, Zhu Y, Li CR, Chen K, Zhao HB. (2020) Hearing loss is an early biomarker in APP/PS1 Alzheimer's disease mice. Neurosci Lett. 717:134705. doi: 10.1016/j.neulet.2019.134705.

Mohr E, Cox C, Williams J, Chase TN, Fedio P (1990) Impairment of central auditory function in Alzheimer's disease. J Clin Exp Neuropsychol 12, 235–246.

Morrison C, Rabipour S, Knoefel F, Sheppard C, Taler V (2018) Auditory event-related potentials in mild cognitive impairment and Alzheimer's disease. Curr Alzheimer Res 15, 702–715.

Murphy C. (2019) Olfactory and other sensory impairments in Alzheimer disease. Nat Rev Neurol. 15:11-24. doi: 10.1038/s41582-018-0097-5.

Ohm TG, Braak H (1989) Auditory brainstem nuclei in Alzheimer's disease. Neurosci Lett 96, 60–63.

Ordóñez-Gutiérrez L, Antón M, Wandosell F. (2015) Peripheral amyloid levels present gender differences associated with aging in AβPP/PS1 mice. J. Alzheimer's Dis. 44: 1063-1068. doi: 10.3233/JAD-141158.

Ordoñez-Gutierrez L, Fernandez-Perez I, Herrera JL, Anton M, Benito-Cuesta I, Wandosell F. (2016) AβPP/PS1 Transgenic Mice Show Sex Differences in the Cerebellum Associated with Aging. J Alzheimers Dis. 54:645-56.

Reiserer RS, Harrison FE, Syverud DC, McDonald MP. (2007). Impaired spatial learning in the APP + PSEN1DeltaE9 bigenic mouse model of Alzheimer's disease. Genes Brain Behav 6(1):54-65

Rochoy M, Rivas V, Chazard E, Decarpentry E, Saudemont G, Hazard PA, Puisieux F, Gautier S, Bordet R. (2019) Factors associated with Alzheimer's disease: An overview of reviews. J Prev Alzheimers Dis. 6:121-134. doi: 10.14283/jpad.2019.7.

Sinha UK, Hollen KM, Rodriguez R, Miller CA (1993) Auditory system degeneration in Alzheimer's disease. Neurology 43, 779–785.

Strouse AL, Hall JW 3rd, Burger MC (1995) Central auditory processing in Alzheimer's disease. Ear Hear 16, 230–238.

Sur S, Sinha VK. (2009) Event-related potential: An overview. Ind Psychiatry J. 18:70-3

Swords GM, Nguyen LT, Mudar RA, Llano DA (2018) Auditory system dysfunction in Alzheimer disease and its prodromal states: A review. Ageing Res Rev 44, 49–59.

Wang XH, Streeter M, Liu YP, Zhao HB. (2009) Identification and characterization of pannexin expression in the mammalian cochlea. J Comp Neurol. 512:336-46.

Weible AP, Stebritz AJ, Wehr M. (2020) 5XFAD mice show early-onset gap encoding deficits in the auditory cortex. Neurobiol Aging. 94:101-110. doi: 10.1016/j.neurobiolaging.2020.05.013. Epub 2020 Jun 1.

Zhao HB, Yu N (2006) Distinct and gradient distributions of connexin26 and connexin30 in the cochlear sensory epithelium of guinea pigs. J Comp Neurol. 499:506-518.

Zheng QY, Johnson K R, Erway LC. (1999) Assessment of hearing in 80 inbred strains of mice by ABR threshold analyses. Hear. Res. 130, 94–107. doi: 10.1016/s0378-5955(99)00003-9

Figure legends:

Fig. 1. Auditory evoked cortex potential (AECP) in CBA/CaJ mice. AECP was evoked by a click stimulus (85 dB SPL) in alternative polarity. Traces were averaged from the recorded mice with both genders. Error bars represents SEM. Mouse age is indicated in each panel. AECP in mice has three positive peaks, i.e., P1, P2, and P3, and corresponding three negative N1, N2, and N3 peaks. Red arrows indicate P3 that is clearly visible in AECP after 3 months old.

Fig. 2. Peak changes of AECP in CBA/CaJ mice with normal aging. AECP was evoked by clicks (85 dB SPL) in alternative polarity. **A:** Time of positive peaks P1, P2, and P3 in AECP at 6 month old. The red lines in boxes represent mean leaves. The peak-time of P1, P2, and P3 is 12.5±2.08, 67.5±2.74, and 128.1±6.76 ms, respectively. **B:** Changes of peak-time in AECP with aging. In comparison with those at age of 3 month old, the peak-times of P2, N2, and P3 in 1 year old mice were significantly reduced. **C-D**: Changes of peak amplitudes with aging. The amplitudes of early waveforms P1, N1, and P2 in AECP reduce with aging, whereas the peaks of later waveforms N2, P3, and N3 have no significant change with aging. *: $P<0.05$, **: $P<0.01$ (t test, two-tail).

Fig. 3. AECP recorded from APP/PS1 AD mice. WT littermates served as control. Mouse age is indicated in each penal. AECP was averaged from the different recorded mice. Red and black traces represent averaged AECP traces recorded from APP/PS1 AD mice and WT mice, respectively. Error bars represents SEM. Blue empty arrows in panel A-B

indicate that P2 peak in AD mice was split. Red arrows indicate P3 that is clearly visible in WT mice but not in AD mice after 4 months old.

Fig. 4. Changes of AECP peaks in APP/PS1 AD mice with aging. WT littermates served as control. Peaks of AECP in each recorded mouse were measured and averaged. P1 and P2 peaks in AD mice are significantly reduced in young age (<6-7 month old) in panel **A-C**, whereas later peaks N2, P3, and N3 appear significant reduction in old ages in penal **D-F**. Penal **E** shows that P3 peak in AD mice are significantly smaller than those in WT mice after 4-month old. *: $P<0.05$, **: $P<0.01$ (t test, two-tail).

Fig. 5. Changes of peak time of AECP in APP/PS1 AD mice with aging. WT littermates served as control. At young age of 1-2 months old, the latencies of N1, P2, and N2 (penal **B-D**) in AD mice are significantly shorter than those in WT mice. At 1 year old, the latencies of peak P1 (penal **A**) and N3 (penal **F**) in AD mice are significantly reduced and the N2 latency (penal **D**) is increased in comparison with those in WT mice. *: $P<0.05$, **: $P<0.01$ (t test, two-tail).

Fig. 6. Comparison of AECP peak changes in CBA/CaJ mice (n=5-6), APP/PS1 AD mice (n=10-21), and WT littermate mice (n=7-15) with aging. **A-C**: Early waveforms (P1, N1, and P2) of AECP in AD mice have significant reduction at the young ages (3 and 6 months old). **D-F:** The peaks of later waveforms (N2, P3, and N3) in APP/PS1 AD mice have significant reduction with aging. P3 in the APP/PS1 AD mice appears significant

reduction after 6 months old. *: P<0.05, **: P<0.01 one-way ANOVA with a Bonferroni correction.

Fig. 7. Expression of amyloid precursor protein (APP) in the auditory cortex (AC) in APP/PS1 AD mice. **A-C:** Immunofluorescent staining of brain slices for APP (red). AC: Auditory cortex. Mice were 2 and 12 months old. **D-E:** High-magnitude images of positive APP-labeling in the AC. Positive labeling for APP is visible at the AC in the 2-month old APP/PS1 AD mouse. White arrows in panel D indicate APP deposits in the AC presented in the typical form of plaques in the 12 months old mouse. Scale bar: 100 μm in **A-C**, 10 μm in **D-E**.

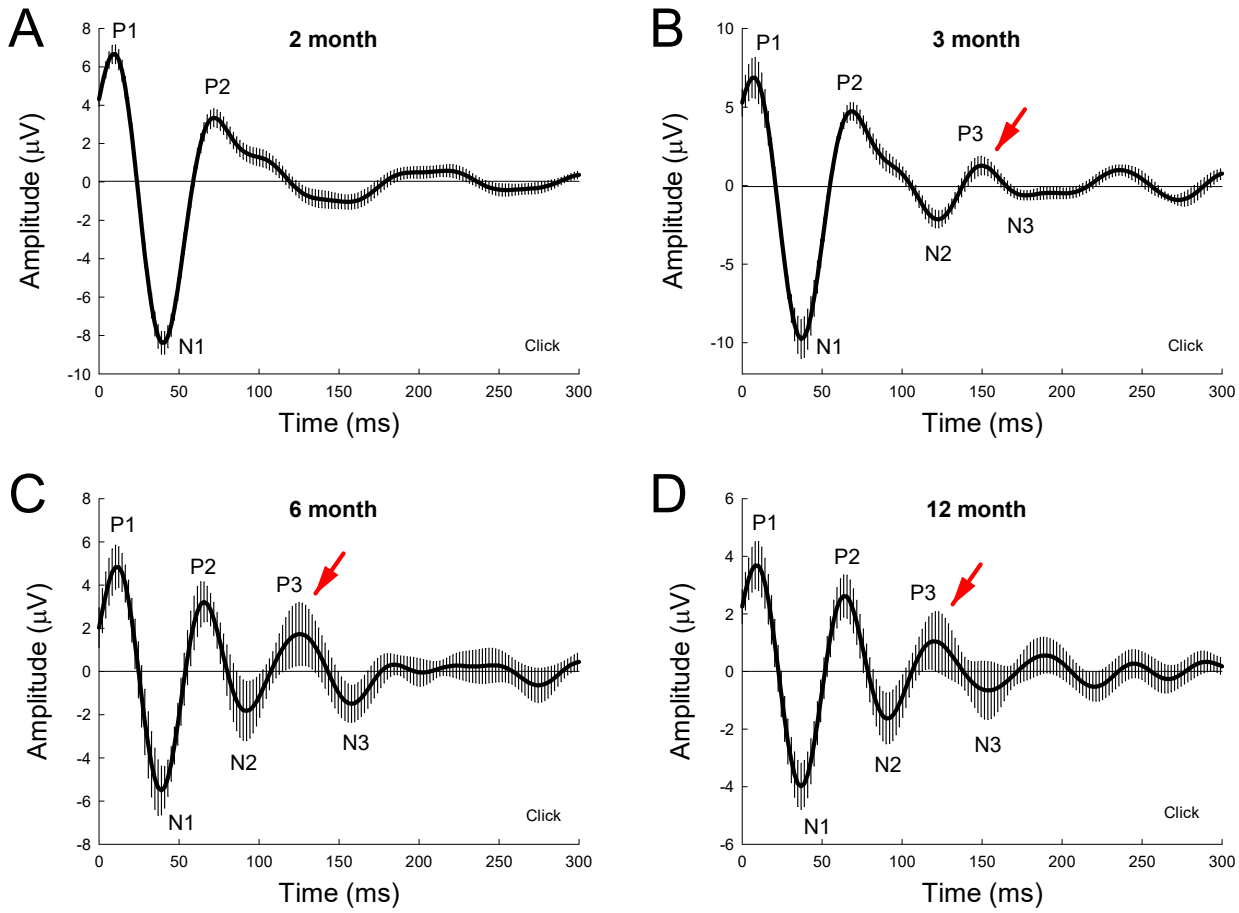

Fig. 1. Auditory evoked cortex potential (AECP) in CBA/CaJ mice. AECP was evoked by a click stimulus (85 dB SPL) in alternative polarity. Traces were averaged from the recorded mice with both genders. Error bars represents SEM. Mouse age is indicated in each panel. AECP in mice has three positive peaks, i.e., P1, P2, and P3, and corresponding three negative N1, N2, and N3 peaks. Red arrows indicate P3 that is clearly visible in AECP after 3 months old.

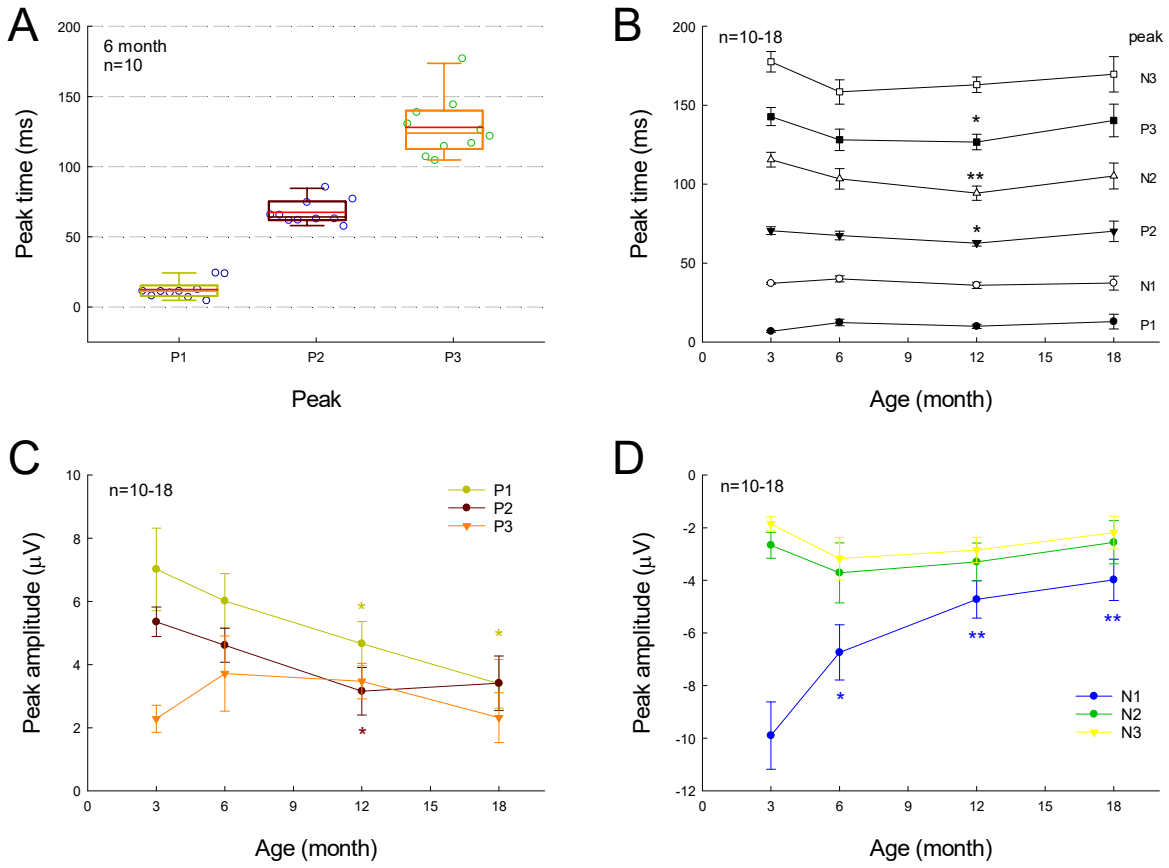

Fig. 2. Peak changes of AECP in CBA/CaJ mice with normal aging. AECP was evoked by clicks (85 dB SPL) in alternative polarity. **A:** Time of positive peaks P1, P2, and P3 in AECP at 6 month old. The red lines in boxes represent mean leaves. The peak-time of P1, P2, and P3 is 12.5±2.08, 67.5±2.74, and 128.1±6.76 ms, respectively. **B:** Changes of peak-time in AECP with aging. In comparison with those at age of 3 month old, the peak-times of P2, N2, and P3 in 1 year old mice were significantly reduced. **C-D**: Changes of peak amplitudes with aging. The amplitudes of early waveforms P1, N1, and P2 in AECP reduce with aging, whereas the peaks of later waveforms N2, P3, and N3 have no significant change with aging. *: $P<0.05$, **: $P<0.01$ (t test, two-tail).

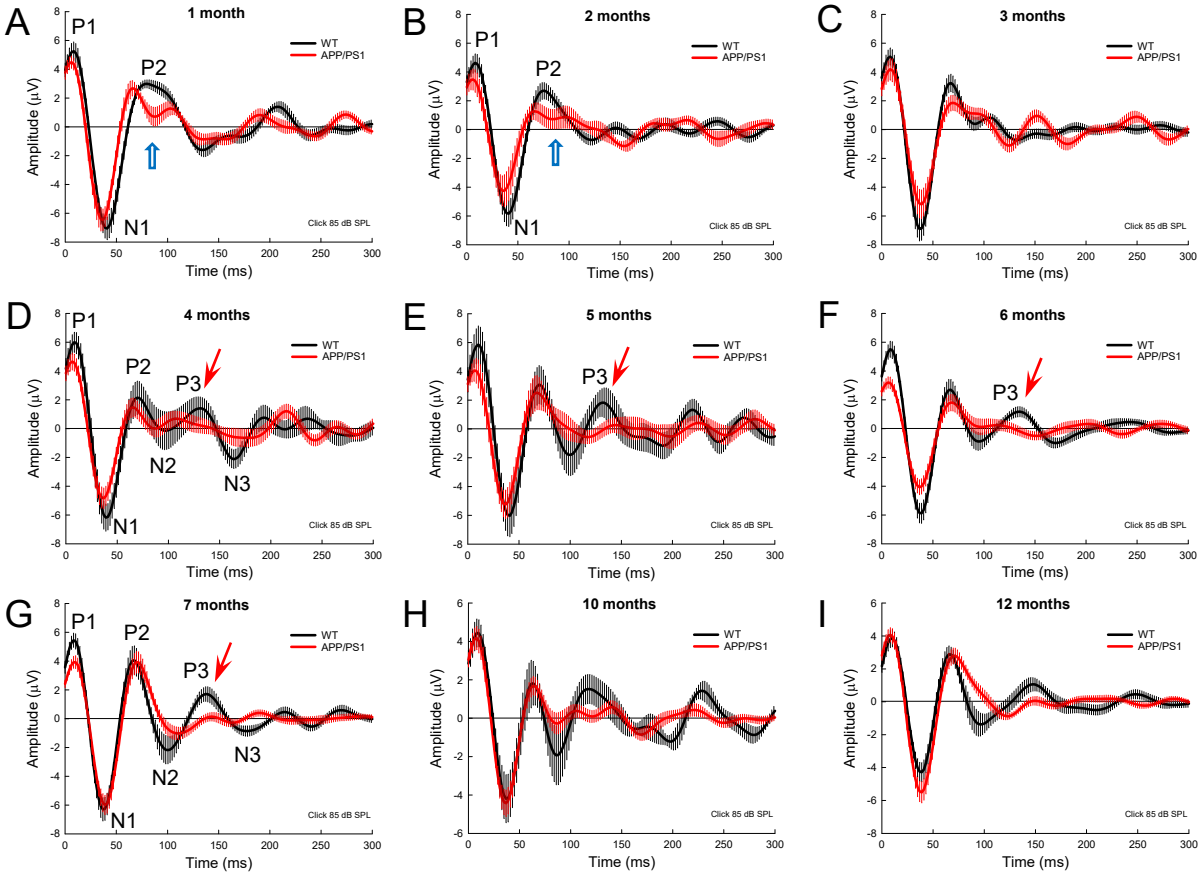

Fig. 3. AECP recorded from APP/PS1 AD mice. WT littermates served as control. Mouse age is indicated in each penal. AECP was averaged from the different recorded mice. Red and black traces represent averaged AECP traces recorded from APP/PS1 AD mice and WT mice, respectively. Error bars represents SEM. Blue empty arrows in panel A-B indicate that P2 peak in AD mice was split. Red arrows indicate P3 that is clearly visible in WT mice but not in AD mice after 4 months old.

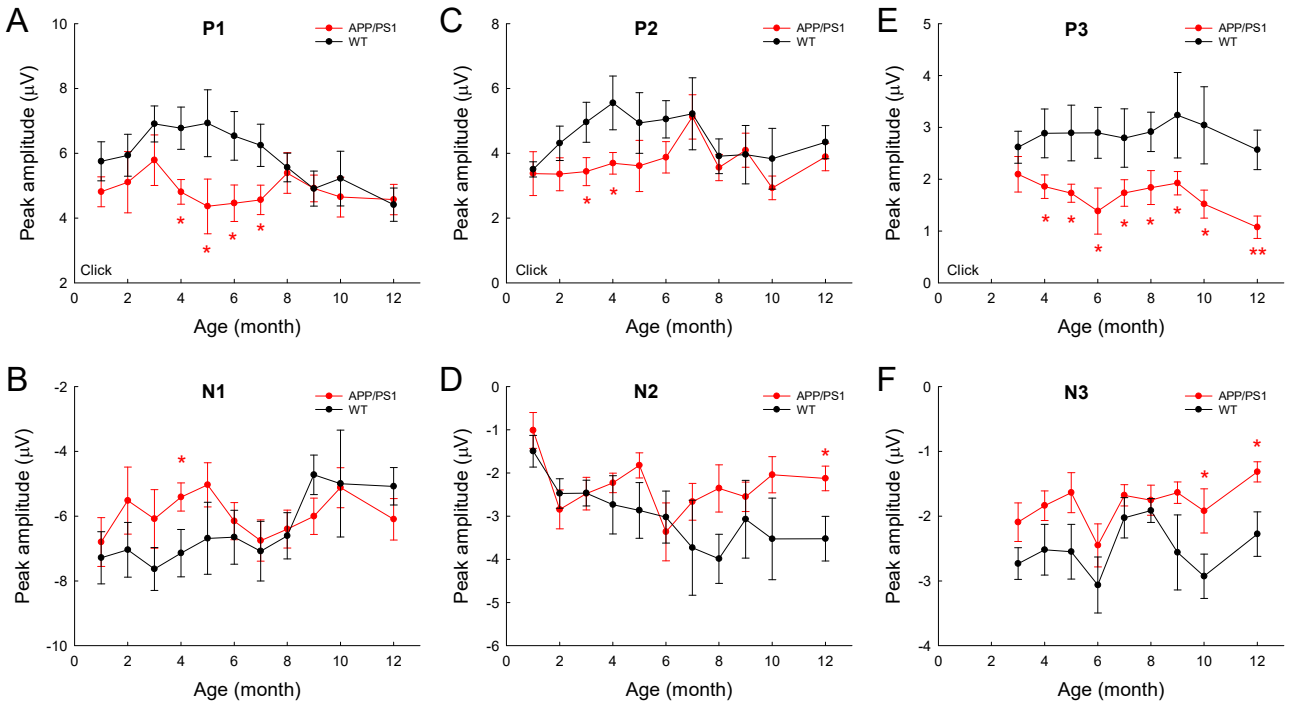

Fig. 4. Changes of AECP peaks in APP/PS1 AD mice with aging. WT littermates served as control. Peaks of AECP in each recorded mouse were measured and averaged. P1 and P2 peaks in AD mice are significantly reduced in young age (<6-7 month old) in panel **A-C**, whereas later peaks N2, P3, and N3 appear significant reduction in old ages in penal **D-F**. Penal **E** shows that P3 peak in AD mice are significantly smaller than those in WT mice after 4-month old. *: P<0.05, **: P<0.01 (t test, two-tail).

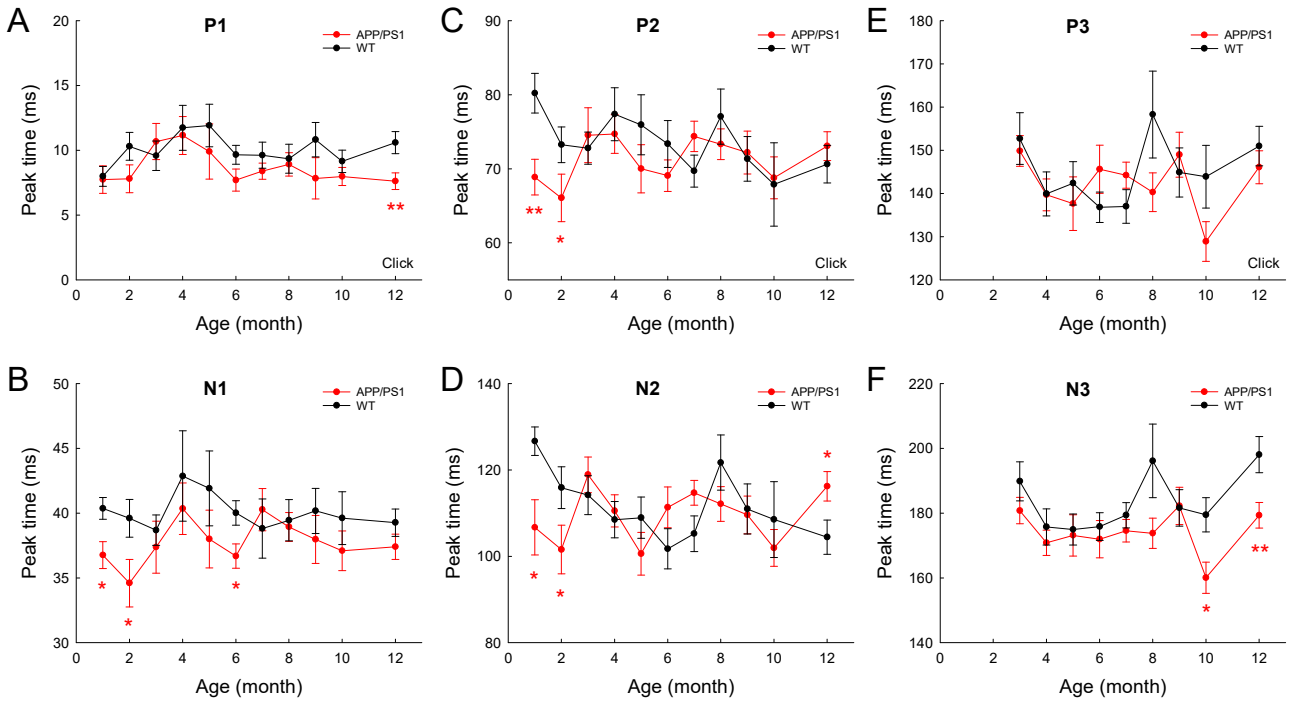

Fig. 5. Changes of peak time of AECP in APP/PS1 AD mice with aging. WT littermates served as control. At young age of 1-2 months old, the latencies of N1, P2, and N2 (penal **B-D**) in AD mice are significantly shorter than those in WT mice. At 1 year old, the latencies of peak P1 (penal **A**) and N3 (penal **F**) in AD mice are significantly reduced and the N2 latency (penal **D**) is increased in comparison with those in WT mice. *: P<0.05, **: P<0.01 (t test, two-tail).

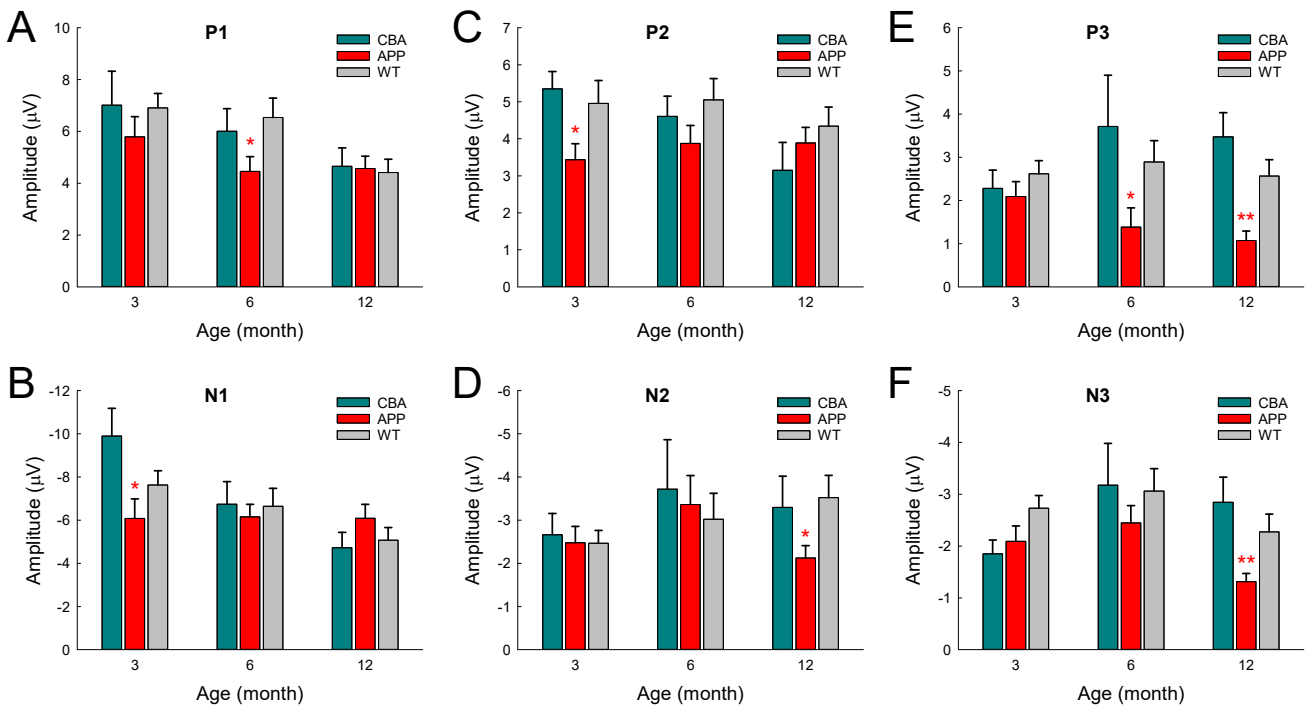

Fig. 6. Comparison of AECP peak changes in CBA/CaJ mice (n=5-6), APP/PS1 AD mice (n=10-21), and WT littermate mice (n=7-15) with aging. **A-C**: Early waveforms (P1, N1, and P2) of AECP in AD mice have significant reduction at the young ages (3 and 6 months old). **D-F:** The peaks of later waveforms (N2, P3, and N3) in APP/PS1 AD mice have significant reduction with aging. P3 in the APP/PS1 AD mice appears significant reduction after 6 months old. *: P<0.05, **: P<0.01 one-way ANOVA with a Bonferroni correction.

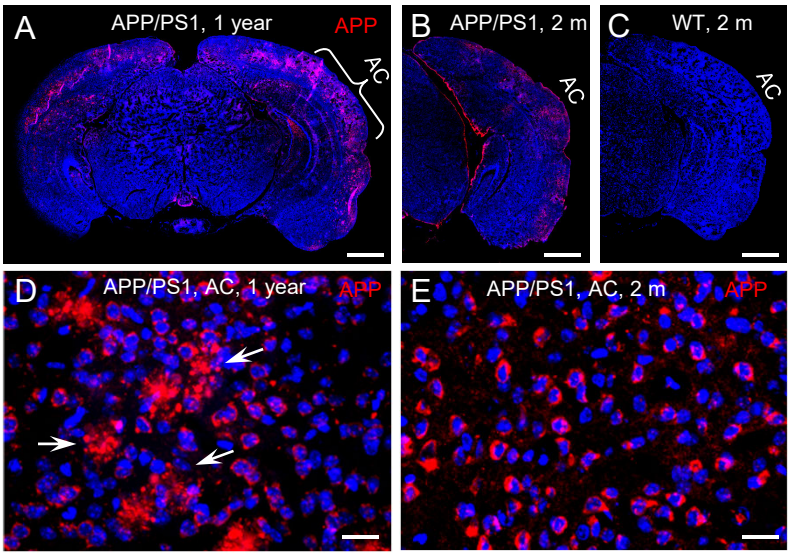

Fig. 7. Expression of amyloid precursor protein (APP) in the auditory cortex (AC) in APP/PS1 AD mice. **A-C:** Immunofluorescent staining of brain slices for APP (red). AC: Auditory cortex. Mice were 2 and 12 months old. **D-E:** High-magnitude images of positive APP-labeling in the AC. Positive labeling for APP is visible at the AC in the 2-month old APP/PS1 AD mouse. White arrows in panel D indicate APP deposits in the AC presented in the typical form of plaques in the 12 months old mouse. Scale bar: 100 μm in **A-C**, 10 μm in **D-E**.